POLITECNICO DI TORINO
Repository ISTITUZIONALE

A bilayer polymer electrolyte encompassing pyrrolidinium-based RTIL for binder-free silicon few-layer graphene nanocomposite anodes for Li-ion battery

Original
A bilayer polymer electrolyte encompassing pyrrolidinium-based RTIL for binder-free silicon few-layer graphene nanocomposite anodes for Li-ion battery / Falco, M., Palumbo, S., Lingua, G., Silvestri, L., Winter, M., Lin, R., Pellegrini, V., Bonaccorso, F., Nair, J.R., Gerbaldi, C.. - In: ELECTROCHEMISTRY COMMUNICATIONS. - ISSN 1388-2481. - STAMPA. - 118:(2020), p. 106807. [10.1016/j.elecom.2020.106807]

Availability:
This version is available at: 11583/2847546 since: 2020-10-05T14:23:32Z

Publisher:
Elsevier Inc.

Published
DOI:10.1016/j.elecom.2020.106807

Terms of use:

This article is made available under terms and conditions as specified in the corresponding bibliographic description in the repository

Publisher copyright

(Article begins on next page)

17 September 2026

Electrochemistry Communications 118 (2020) 106807

Contents lists available at ScienceDirect

Electrochemistry Communications

journal homepage: www.elsevier.com/locate/elecom

A bilayer polymer electrolyte encompassing pyrrolidinium-based RTIL for binder-free silicon few-layer graphene nanocomposite anodes for Li-ion battery

M. Falco[a,*], S. Palumbo[b,c], G. Lingua[a], L. Silvestri[b,d], M. Winter[e], R. Lin[f], V. Pellegrini[g,b], F. Bonaccorso[g,b], Jijeesh R. Nair[e], C. Gerbaldi[a,*]

[a] GAME Lab, Department of Applied Science and Technology (DISAT), Politecnico di Torino, Corso Duca degli Abruzzi 24, 10129 Torino, Italy
[b] Istituto Italiano di Tecnologia, IIT, Graphene Labs, Via Morego 30, 16163 Genova, Italy
[c] Istituto Nazionale di Ricerca Metrologica, INRIM, Department of Metrology for Quality of Life, Strada delle Cacce 91, 10135 Torino, Italy
[d] ENEA C.R. Casaccia, Energy Department, Via Anguillarese 301, 00123 Roma, Italy
[e] Helmholtz-Institute Münster (HI MS), IEK-12, Forschungszentrum Jülich GmbH, and MEET Battery Research Center, University of Münster, Corrensstraße 46, 48149 Münster, Germany
[f] Solvionic SA, Site Bioparc Sanofi, 195 Route d'Espagne BP1169, 31036 Toulouse Cedex 1, France
[g] Bedimensional Spa Genova, Via Albisola 79, 16163 Genova, Italy

ARTICLE INFO

Keywords:
Li-ion battery
Polymer electrolyte
Silicon anode
Graphene
Ionic liquid

ABSTRACT

A binder-free electrode made of polycrystalline carbon-coated silicon nanoparticles encapsulated in few-layer graphene flakes is coupled with a PEO-based crosslinked bilayer polymer electrolyte (BLPE). A soft polymer electrolyte layer enriched with a pyrrolidium-based ionic liquid (Pyr_{14}TFSI) is deposited on top of the electrode and UV cured by an *in situ process* to achieve optimal interfacial contact. A hard layer consisting of a crosslinked PEO-based polymer electrolyte film with a lower amount of Pyr_{14}TFSI is integrated with the electrode/electrolyte assembly to improve the self-standing and shape-retention abilities. Proof-of-concept lab-scale Si-C||Li-metal polymer cells demonstrate a reversible specific discharge capacity up to 1044 mAh g_{Si}^{-1} at 80 °C, largely outperforming the one with Pyr_{14}TFSI/LiTFSI liquid electrolyte under the same experimental condition. Our results highlight the beneficial effect of the crosslinked PEO-based polymer matrix on the cycling performance, despite the absence of any SEI-forming agent.

1. Introduction

The quest for Li-ion batteries (LIBs) with high energy density, chiefly for application in electric vehicles, calls for anode materials with improved practical specific capacity as compared to the theoretical capacity of 372 mAh g^{-1} of graphite [1,2]. Overcoming limitations of organic carbonate-based liquid electrolytes due to the complex interfacial chemistry and flammability is also fundamental in designing safer LIBs [3]. In this regard, research efforts are devoted to replace the liquid electrolytes with highly-conductive solid electrolytes aiming to improve cycle life, obtain compact stacks without separators and reduce the countermeasures commonly used to ensure safety [4,5]. To address these issues, a high-capacity Si-based anode (theoretical capacity 3579 mAh g^{-1}) [6] and safe crosslinked polymer electrolytes encompassing room temperature ionic liquids (RTILs) are herein proposed.

The development of Si anodes faces major issues related to the large expansion/contraction upon lithiation/delithiation (> 300%) leading to Si pulverization, electrical contact loss, disruption of the solid electrolyte interphase (SEI) and, eventually, cell failure [7,8]. To this end, nanosized Si, combined with carbon in Si-C composites, is extensively investigated to enhance conductivity and mitigate pulverization. Among the C-based components, highly electronically conducting and elastic 2D structured materials like graphene are particularly effective in buffering extreme volume variations [2,8]. A facile method for the preparation of composite electrodes comprising few-layer graphene (FLG) embedding Si nanoparticles (Si-NPs) was proposed [9,10]. The resulting binder-free Si-FLG electrodes already demonstrated excellent electrochemical performances, achieving high specific capacity (> 1800 mAh g_{Si}^{-1}) and Coulombic efficiency (CE ≈ 99%) in lab-scale cells. These results were obtained with a reference electrolyte (LP30:

* Corresponding authors at: GAME Lab, Department of Applied Science and Technology (DISAT), Politecnico di Torino, Corso Duca degli Abruzzi 24, 10129 Torino, Italy.
E-mail addresses: marisa.falco@polito.it (M. Falco), claudio.gerbaldi@polito.it (C. Gerbaldi).

https://doi.org/10.1016/j.elecom.2020.106807
Received 9 June 2020; Received in revised form 17 July 2020; Accepted 22 July 2020
Available online 26 July 2020
1388-2481/ © 2020 The Author(s). Published by Elsevier B.V. This is an open access article under the CC BY-NC-ND license (http://creativecommons.org/licenses/BY-NC-ND/4.0/).

1 M $LiPF_6$ in a 50/50 v/v mixture of DMC/EC) added with 10% (v/v) of fluoroethylene carbonate (FEC) [10].

FEC is one of the most effective SEI-forming agents for Si-based anodes, due to its ability to form thin and dense passivation layers rich in inorganic fluorides [11]. In this regard, RTILs with bis(trifluorosulfonyl)imide anion ($TFSI^-$) have been found to have poor SEI-film forming ability, particularly when compared to their bis(fluorosulfonyl)imide (FSI^-) based counterparts [12,13]. Nevertheless, there are several reports of Si-based anodes working with $TFSI^-$ based RTILs, which points at the fundamental role of each peculiar electrode material composition and morphology in determining the SEI quality and the cell performance [14]. RTILs are widely investigated as electrolyte components in LIBs, mainly due to their non-flammability, high ionic conductivity, excellent electrochemical and thermal stabilities [15]. Accordingly, advances in the synthesis method are leading to eco-friendly and low-cost processes to enable scalability [16].

In this work, we present a bilayer polymer electrolyte (BLPE) that combines $Pyr_{14}TFSI$ and LiTFSI with a poly(ethylene oxide) (PEO)-based crosslinked polymer host to deliver a solid-state Li polymer cell. Additives that are commonly used for Si-anodes, such as FEC and vinylene carbonate (VC) are not used in this BLPE. Direct *in situ* deposition and crosslinking [17] onto the binder-free Si-FLG electrode is exploited to achieve an intimate electrode|electrolyte interface and enhance the electrochemical performance as compared to liquid $Pyr_{14}TFSI$/LiTFSI.

2. Experimental procedures

Binder-free Si-FLG composite electrodes were prepared using Si-NPs (< 100 nm, Alfa Aesar) and FLG flakes obtained by wet-jet milling exfoliation of graphite (+100 mesh, Aldrich), following a previously reported procedure [9,10]. Briefly, equal masses of Si-NPs, FLG and poly(acrylic acid) (PAA) were dispersed in ethanol, followed by ultrasonication for 90 min. The obtained dispersion was deposited onto a copper disk (Ø 18 mm) by drop casting and dried in air. The resulting film was annealed in a tubular furnace under a reducing atmosphere (vacuum + 5 sccm of H_2) for 30 min at 750 °C (heating rate 15 °C min^{-1} up to 700 °C, and 5 °C min^{-1} to reach 750 °C). The resulting composite electrode has a Si content of 57% by weight, corresponding to a Si mass loading of 0.28 ± 0.04 mg cm^{-2}.

To prepare the RTIL-based liquid electrolyte (IL_liq), $Pyr_{14}TFSI$ and LiTFSI (battery grade, Solvionic) were mixed under stirring at a 6:1 molar ratio, respectively. To obtain the RTIL-rich "soft" polymer electrolyte layer (PEO-SL), IL_liq, PEO (Mn 200000 Da, Aldrich, vacuum dried 48 h/50 °C) and benzophenone (BP, Aldrich) were homogenized into a paste at 70 °C. BP is a hydrogen-abstracting photoinitiator, which induces crosslinking between polymer chains [17,18]. The weight percentages of IL_liq, PEO and BP are 78.3, 20.7 and 1.0, respectively. To obtain the electrode/electrolyte composite (Si-FLG/PEO-SL), PEO-SL paste was deposited on the Si-FLG electrode and hot-pressed (10 bar, 70 °C) between two polypropylene (PP) sheets, using ≈ 60 μm spacers for thickness control. The resulting Si-FLG/PEO-SL composite was crosslinked for 1.5 min under UV light (UV-curing) using a medium pressure Hg lamp (Helios Italquartz), and detached from the PP sheets. To prepare the "hard" polymer electrolyte film (PEO-HL), LiTFSI, $Pyr_{14}TFSI$, PEO and BP (15.8, 41.1, 41.1 and 2.0 wt%, respectively) were homogenized into a paste at 70 °C. In both PEO-SL and PEO-HL, the EO/Li molar ratio is 17. The PEO-HL paste was placed between two PP sheets with spacers, and processed into a film by hot-pressing (70 °C, 10 bar) and UV-curing for 1.5 min in order to peel-off one of the PP sheets. The PEO-HL film was sandwiched with the Si-FLG/PEO-SL electrode/electrolyte composite, and the resulting Si-FLG/BLPE assembly was sealed under vacuum to guarantee optimal contact between the components. Si-FLG/BLPE was then UV-cured for 3 min to join the polymer layers and finally cut into a 20 mm diameter disk (to avoid any short circuit, as the Si-FLG disk has Ø18 mm). The BLPE for the ionic conductivity measurement was prepared following the same procedure used for Si-FLG/BLPE, but no electrode was used in this case.

The Si-FLG/BLPE was assembled in an ECC-Std cell (EL-cell, Germany) with a 18 mm Li metal disk anode (200 μm thick, Albermarle) in a two-electrodes configuration. The Li||Si-FLG cell with IL_liq was assembled using a glass wool Whatman separator drenched with 200 μL of electrolyte. Test cells were galvanostatically cycled (GC) at 80 °C with an Arbin BT2000 battery tester, between 0.01 and 2 (1st cycle) and 0.1–1 V (subsequent cycles), at 250 mA g_{Si}^{-1}, based on the maximum practical capacity of the electrode material (≈2500 mAh g_{Si}^{-1}, in the 0.1–1 V range) [7]. The specific capacities are based on the amount of Si in the electrodes. The ionic conductivity was obtained from electrochemical impedance spectroscopy (EIS, freq. range 300 KHz – 1 Hz, V_{AC} = 20 mV) on a VMP3 workstation (Biologic), using stainless steel (SS) electrodes in symmetric SS|PEO-HL|SS ECC-Std cells. The spectra were collected at 10 °C intervals between −20 and 80 °C, inside an environmental simulation chamber (MK-53, Binder), with 1.5 h equilibration time at each temperature. Electrolyte preparation and cell assembly were carried out in an Ar-filled glove box (Jacomex GP2, O_2/H_2O < 1 ppm). Hot-pressing and UV-curing were carried out in transparent bags sealed under vacuum. Viscosity (η) measurement was carried out on an Anton Paar MCR 102 device in rotation mode using a cone (15 mm) and plate technique (60 °C at 100 rpm). The glass transition temperature (T_g) was evaluated by differential scanning calorimetry (DSC) during the second heating cycle between −150 and 220 °C (N_2 flow, heating rate 10 °C min^{-1}) using DSC 2500 by TA instruments. Morphological analysis was carried out with a VEGA3 TESCAN Scanning Electron Microscope (SEM) equipped with an Energy-Dispersive X-ray microanalysis (EDX).

3. Results and discussion

Fig. 1a shows the ionic conductivity data extracted from EIS of symmetric SS|BLPE|SS cells. The BLPE film shows a high ionic conductivity of 0.1 and 1.4 mS cm^{-1} at 30 and 60 °C, respectively.

The Si-FLG electrode preparation includes a thermal treatment under reducing condition, allowing the pyrolysis (carbonization) of PAA, thus increasing electronic conductivity and binding between Si-NPs and FLG flakes. The resulting binder-free nanostructured Si-FLG comprises horizontally oriented FLG flakes entrapping the Si-NPs (Fig. 1b, more details and complete characterization of the Si-FLG electrode in [7]). As for enhancing active material utilization, an innovative bilayer polymer electrolyte concept is attempted here. Both polymer electrolyte layers consist of PEO, $Pyr_{14}TFSI$, LiTFSI, and a photoinitiator; the "soft" PEO-SL component contains more RTIL (70.3 wt%) than its "hard" PEO-HL (41.1 wt%) counterpart. The lower η at 60 °C of the PEO-SL precursor (31.6 Pa s) as compared to PEO-HL (200 Pa s) allows for the direct deposition on top of the Si-FLG electrode and *in situ* crosslinking (Fig. 1c-1, [17]), enabling the penetration of the paste through the open structure and voids of the electrode film, as confirmed by cross-sectional SEM analysis (Fig. 1d, e) and elemental maps (Fig. 1f, g). Due to the high amount of $Pyr_{14}TFSI$, PEO-SL (EO/RTIL = 10/3.5 by mol, T_g = −77.4 °C) is a sticky film that loses its mechanical properties upon elongation, consistent with the literature about crosslinked PEO-based systems at high RTIL content (e.g. at EO/RTIL = 10/4 by mol) [18]. Therefore, PEO-HL layer (EO/RTIL = 10/1 by mol, T_g = −63.2 °C) was finally integrated to the Si-FLG|PEO-SL followed by UV-curing, to confer mechanical integrity, yielding the Si-FLG|BLPE assembly (scheme of Fig. 1c) as detailed in the experimental section. After UV-curing it results in a thermoset shape-retaining elastic film with self-standing ability (Fig. 1c-2).

Fig. 2a shows the voltage vs. specific capacity profiles upon GC of the proof-of-concept Si-FLG|BLPE|Li cell. During the first cycle, the lower cut-off voltage was set to 0.01 V, to ensure proper amorphization of polycrystalline Si [10]. The shoulder at ≈0.7 V (inset to Fig. 2a) during the first charge (lithiation) probably accounts for the partial

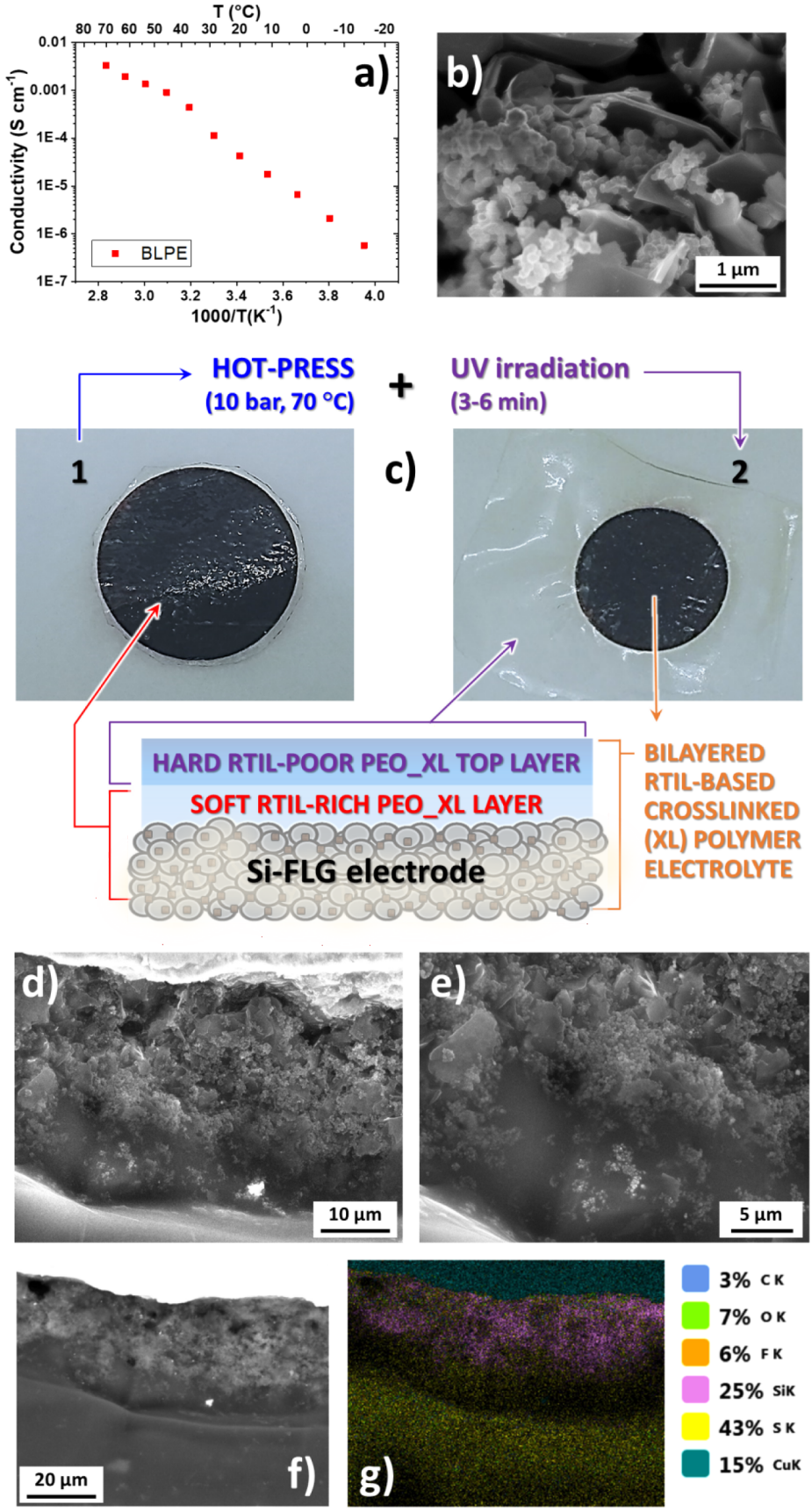

Fig. 1. a) Arrhenius plot of ionic conductivity vs. T of BLPE bilayer polymer electrolyte. b) SEM images of the Si-FLG electrode at different magnifications. c) Digital photographs of crosslinked Si-FLG/PEO-SL electrode/"soft" electrolyte composite (1) and Si-FLG/BLPE electrode/bilayer electrolyte assembly (2), with related sketched scheme below. d, e) Cross-sectional SEM images of Si-FLG/BLPE at different magnifications, and f, g) corresponding EDX elemental maps.

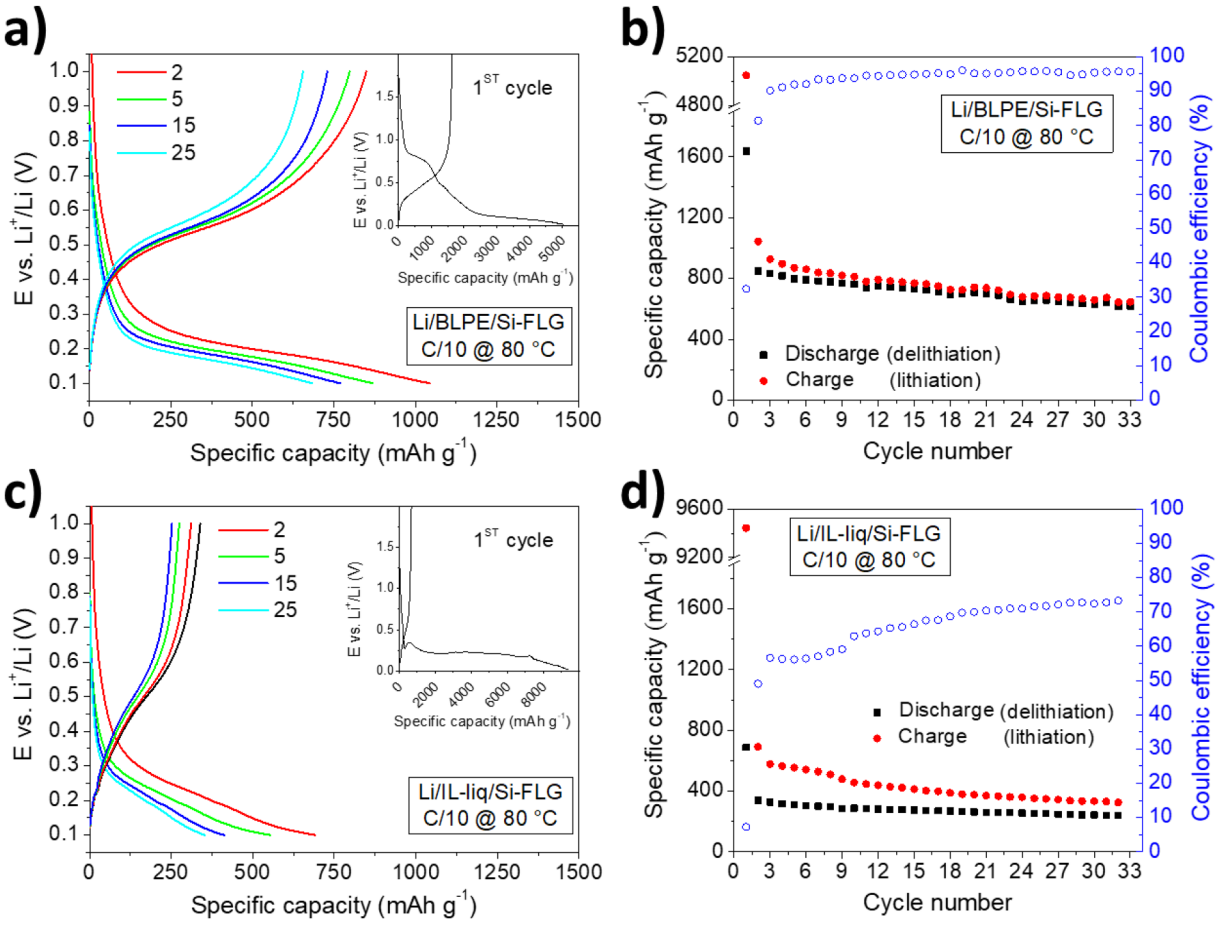

Fig. 2. Voltage vs. specific capacity profiles for selected cycles of Si-FLG|BLPE|Li (a) and Si-FLG|IL_liq|Li (c) cells and (b, d) their respective plots of specific capacity and CE vs. cycle number.

degradation of electrolyte components, leading to a CE of 32% in the first cycle (Fig. 2b). The intercalation of Pyr_{14}^{+} into the FLG may take place, similarly to what occurs in Li||graphite cells with Pyr_{14}TFSI/LiTFSI-based electrolytes at 0.9 and 0.5 V according to the literature [19]. Nevertheless, the specific capacity delivered upon discharge (delithiation) is as high as 1637 mAh g_{Si}^{-1}. Despite additional optimization work is clearly needed to improve the initial CE with the polymer electrolyte [20], it is worth noting that under the same cycling conditions, the cell with IL_liq delivers 687 mAh g_{Si}^{-1} upon discharge, with an initial CE of 7% (Fig. 2c). In this latter, the profile for the first discharge (inset to Fig. 2c) shows an irregular plateau at ~0.2 V, suggesting a prolonged degradation process.

In the following cycles, the cut-off voltage window of Si-FLG|BLPE|Li cell was reduced to 0.1–1 V to improve the cycling ability at the expense of the practical specific capacity (from 3500 to ≈2300 mAh g_{Si}^{-1}) [10]. In this range, the Si-FLG|BLPE|Li cell delivers a maximum discharge capacity of 1044 mAh g_{Si}^{-1}, with a capacity retention of 65% after more than 30 cycles (Fig. 2b). The CE is stabilized at > 95% after 10 cycles. Under the same cycling condition, the IL_liq-based cell shows charge capacity values of 692 and 334 mAh g_{Si}^{-1}, with CEs of 49 and 72% at the 2nd and 30th cycle, respectively (Fig. 2d). This result is consistent with literature reports that account for poor cycling performance of Si-based anodes with RTILs containing $TFSI^{-}$ [12,21]. Here, the crosslinked PEO matrix provides a protective function, preventing major degradation processes due to RTIL. This is likely related to the formation of a more effective SEI-passivation layer in the co-presence of PEO [22,23]. Alternatively, the effect of PEO might be related to a change in the coordination of Li^{+}, damping down the irreversible decomposition of the electrolyte due to the interactions with FLG, similarly to what observed with oxygen-containing binders preventing the intercalation of Pyr_{14}^{+} into graphite according to the literature [24].

4. Conclusion

The first example of a nanostructured binder-free electrode comprising Si-NPs encapsulated within few-layer graphene flakes combined with a crosslinked PEO-based bilayer polymer electrolyte containing Pyr_{14}TFSI is here presented. The bilayer concept enables direct *in situ* polymerization to achieve excellent inter-penetration between the active material and the polymer electrolyte while ensuring shape-retention ability upon thermal stress, accounting for enhanced safety.

As a result, despite the absence of any specific SEI-forming additive, a proof-of-concept Li-metal polymer cell demonstrates a reversible specific capacity of 1044 mAh g_{Si}^{-1} upon charge, with higher CE, specific capacity and capacity retention as compared to its liquid RTIL-based counterpart. The UV-crosslinked BLPE concept proves to be effective in preventing substantial degradation observed with the RTIL-based liquid electrolyte, which along with the remarkable preliminary electrochemical results, demonstrates its potential for the use in high-performance and versatile Li-metal polymer batteries.

CRediT authorship contribution statement

M. Falco: Conceptualization, Methodology, Investigation, Data curation, Validation, Formal analysis, Writing - original draft, Writing - review & editing. **S. Palumbo:** Investigation, Validation, Writing - review & editing. **G. Lingua:** Investigation, Validation, Visualization,

Writing - review & editing. **L. Silvestri:** Methodology, Investigation, Data curation, Writing - review & editing. **M. Winter:** Supervision, Project administration, Funding acquisition. **R. Lin:** Resources, Validation. **V. Pellegrini:** Supervision, Project administration, Funding acquisition, Writing - review & editing. **F. Bonaccorso:** Methodology, Writing - review & editing. **Jijeesh R. Nair:** Conceptualization, Investigation, Validation, Writing - review & editing. **C. Gerbaldi:** Conceptualization, Visualization, Supervision, Writing - original draft, Writing - review & editing, Project administration, Funding acquisition.

Declaration of Competing Interest

The authors declare that they have no known competing financial interests or personal relationships that could have appeared to influence the work reported in this paper.

Acknowledgements

M.F., G.L. and C.G. acknowledge financial support by the Si-DRIVE Project, which received funding from the EU's Horizon 2020 research and innovation (R&I) programme under GA 814464. The ENABLES project received funding from the EU's H2020 (R&I) programme under GA 730957. V.P., L.S., S.P. and F.B., acknowledge the EU's H2020 (R&I) program under GA 785219–GrapheneCore2. M.W. and J.R.N. acknowledge the support provided by the German Federal Ministry of Education and Research within the (BMBF) project "FestBatt" (13XP0175A). The authors are grateful to Livia Della Seta from Energy Department at ENEA C.R. Casaccia for SEM imaging.

References

[1] R. Schmuch, R. Wagner, G. Hoerpel, T. Placke, M. Winter, Performance and cost of materials for lithium-based rechargeable automotive batteries, Nat. Energy 4 (2018) 267, https://doi.org/10.1038/s41560-018-0107-2.

[2] E. Pomerantseva, F. Bonaccorso, X. Feng, Y. Cui, Y. Gogotsi, Energy storage: The future enabled by nanomaterials, Science 366 (2019) 8285, https://doi.org/10.1126/science.aan8285.

[3] F.H. Gandoman, J. Jaguemont, S. Goutam, R. Gopalakrishnan, Y. Firouz, T. Kalogiannis, N. Omar, J. Van Mierlo, Concept of reliability and safety assessment of Li-ion batteries in electric vehicles: basics, progress and challenges, Appl. Energy 251 (2019) 113343, , https://doi.org/10.1016/j.apenergy.2019.113343.

[4] J.R. Nair, L. Imholt, G. Brunklaus, M. Winter, Lithium metal polymer electrolyte batteries: opportunities and challenges, Electrochem. Soc. Interface 28 (2020) 55, https://doi.org/10.1149/2.F05192if.

[5] J. Schnell, T. Günther, T. Knoche, C. Vieider, L. Köhler, A. Just, M. Keller, S. Passerini, G. Reinhart, All-solid-state Li-ion and Li metal batteries: paving the way to large-scale production, J. Power Sources 382 (2018) 160–175, https://doi.org/10.1016/j.jpowsour.2018.02.062.

[6] S. Chae, S.-H. Choi, N. Kim, J. Sung, J. Cho, Integration of graphite and silicon anodes for the commercialization of high-energy lithium-ion batteries, Angew. Chem. Int. Ed. 59 (2020) 110–135, https://doi.org/10.1002/anie.201902085.

[7] M. Winter, W.K. Appel, B. Evers, T. Hodal, K.C. Moeller, I. Schneider, M. Wachtler, M.R. Wagner, G.H. Wrodnigg, J.O. Besenhard, Studies on the anode/electrolyte interface in lithium ion batteries, Chem. Mon. 132 (2001) 473, https://doi.org/10.1007/s007060170110.

[8] F. Dou, L. Shi, G. Chen, D. Zhang, Si/C composite anodes for Li-ion batteries, Electrochem. Energy Rev. 2 (2019) 149–198, https://doi.org/10.1007/s41918-018-00028-w.

[9] E. Greco, G. Nava, R. Fathi, F. Fumagalli, A.E. Del Rio-Castillo, A. Ansaldo, F. Di Fonzo, S. Monaco, F. Bonaccorso, V. Pellegrini, Few-layer graphene improves Si performance in Li-ion battery anodes, J. Mater. Chem. A 5 (2017) 19306–19315, https://doi.org/10.1039/C7TA05395A.

[10] S. Palumbo, L. Silvestri, A. Ansaldo, R. Brescia, F. Bonaccorso, V. Pellegrini, Si few-layer graphene nanocomposite as high-capacity and high-rate anode in Li-ion batteries, ACS Appl. Energy Mater. 2 (2019) 1793–1802, https://doi.org/10.1021/acsaem.8b01927.

[11] G.G. Eshetu, E. Figgemeier, Confronting the challenges of next-generation silicon anode-based Li-ion batteries: role of designer electrolyte additives and polymeric binders, ChemSusChem 12 (2019) 2515–2539, https://doi.org/10.1002/cssc.201900209.

[12] D.M. Piper, T. Evans, K. Leung, T. Watkins, J. Olson, S.C. Kim, S.S. Han, V. Bhat, K.H. Oh, D.A. Buttry, S.-H. Lee, Stable Si-ionic liquid interface for next-gen Li-ion batteries, Nat. Comm. 6 (2015) 6230, https://doi.org/10.1038/ncomms7230.

[13] L. Grande, J. von Zamory, S.L. Koch, J. Kalhoff, E. Paillard, S. Passerini, Homogeneous Li electrodeposition with pyrrolidinium-based ionic liquid electrolytes, ACS Appl. Mater. Interfaces 7 (2015) 5950–5958, https://doi.org/10.1021/acsami.5b00209.

[14] S. Zhang, M. He, C.-C. Su, Z. Zhang, Advanced electrolyte/additive for Li-ion batteries with Si anode, Curr. Opin. Chem. Eng. 13 (2016) 24–35, https://doi.org/10.1016/j.coche.2016.08.003.

[15] Q. Yang, Z. Zhang, X.-G. Sun, Y.-S. Hu, H. Xing, S. Dai, Ionic liquids and derived materials for Li and Na batteries, Chem. Soc. Rev. 47 (2018) 2020–2064, https://doi.org/10.1039/C7CS00464H.

[16] E. Simonetti, M. De Francesco, M. Bellusci, G.T. Kim, F. Wu, S. Passerini, G.B. Appetecchi, A more sustainable and cheaper one-pot route for the synthesis of hydrophobic ionic liquids for electrolyte applications, ChemSusChem 12 (2019) 4946–4952, https://doi.org/10.1002/cssc.201902054.

[17] L. Porcarelli, C. Gerbaldi, F. Bella, J.R. Nair, Super soft all-ethylene oxide polymer electrolyte for safe all-solid Li batteries, Sci. Rep. 6 (2016) 19892, https://doi.org/10.1038/srep19892.

[18] G.T. Kim, G.B. Appetecchi, M. Carewska, M. Joost, A. Balducci, M. Winter, S. Passerini, UV cross-linked, lithium-conducting ternary polymer electrolytes containing ionic liquids, J. Power Sources 195 (2010) 6130–6137, https://doi.org/10.1016/j.jpowsour.2009.10.079.

[19] M. Nádherná, J. Reiter, J. Moškon, R. Dominko, Lithium bis (fluorosulfonyl) imide–$PY_{R1}4$TFSI ionic liquid electrolyte compatible with graphite, J. Power Sources 196 (2011) 7700–7706, https://doi.org/10.1016/j.jpowsour.2011.04.033.

[20] F. Zhang, J. Yang, Boosting initial coulombic efficiency of Si-based anodes: a review, Emergent Mater. (2020), https://doi.org/10.1007/s42247-020-00080-7.

[21] T. Sugimoto, Y. Atsumi, M. Kono, M. Kikuta, E. Ishiko, M. Yamagata, M. Ishikawa, Application of bis(fluorosulfonyl)imide-based ionic liquid electrolyte to silicon–nickel–carbon composite anode for Li-ion batteries, J. Power Sources 195 (2010) 6153–6156, https://doi.org/10.1016/j.jpowsour.2010.01.011.

[22] Y. Jin, N.J.H. Kneusels, L.E. Marbella, E. Castillo-Martínez, P.C. Magusin, R.S. Weatherup, E. Jónsson, T. Liu, S. Paul, C.P. Grey, Understanding fluoroethylene carbonate and vinylene carbonate based electrolytes for Si anodes in Li-ion batteries with NMR spectroscopy, J. Am. Chem. Soc. 140 (2018) 9854–9867, https://doi.org/10.1021/jacs.8b03408.

[23] C.K. Chan, R. Ruffo, S.S. Hong, Y. Cui, Surface chemistry and morphology of the solid electrolyte interphase on silicon nanowire Li-ion battery anodes, J. Power Sources 189 (2009) 1132–1140, https://doi.org/10.1016/j.jpowsour.2009.01.007.

[24] S. Komaba, N. Yabuuchi, T. Ozeki, K. Okushi, H. Yui, K. Konno, Y. Katayama, T. Miura, Functional binders for reversible lithium intercalation into graphite in propylene carbonate and ionic liquid media, J. Power Sources 195 (2010) 6069–6074, https://doi.org/10.1016/j.jpowsour.2009.12.058.